An InGaAlAs–InGaAs Two-Color Photodetector for Ratio Thermometry

Xinxin Zhou, Matthew J. Hobbs, Benjamin S. White, John P. R. David, *Fellow, IEEE*, Jon R. Willmott, and Chee Hing Tan, *Member, IEEE*

***Abstract*— We report the evaluation of a molecular-beam epitaxy grown two-color photodetector for radiation thermometry. This two-color photodetector consists of two p^+in^+ diodes, an $In_{0.53}Ga_{0.25}Al_{0.22}As$ (hereafter InGaAlAs) p^+in^+ diode, which has a cutoff wavelength of 1180 nm, and an $In_{0.53}Ga_{0.47}As$ (hereafter InGaAs) p^+in^+ diode with a cutoff wavelength of 1700 nm. Our simple monolithic integrated two-color photodetector achieved comparable output signal and signal-to-noise (SNR) ratio to that of a commercial two-color Si-InGaAs photodetector. The InGaAlAs and InGaAs diodes detect blackbody temperature as low as 275 °C and 125 °C, respectively, with an SNR above 10. The temperature errors extracted from our data are 4 °C at 275 °C for the InGaAlAs diode and 2.3 °C at 125 °C for the InGaAs diode. As a ratio thermometer, our two-color photodetector achieves a temperature error of 12.8 °C at 275 °C, but this improves with temperature to 0.1 °C at 450 °C. These results demonstrated the potential of InGaAlAs–InGaAs two-color photodetector for the development of high performance two-color array detectors for radiation thermometry and thermal imaging of hot objects.**

***Index Terms*— Radiation thermometry, temperature measurement, two-color photodetector.**

I. Introduction

RADIATION thermometers are widely used in noncontact temperature measurement systems where the target is inaccessible, for example, due to the extremely high temperatures in a blast furnace or to prevent contamination in semiconductor wafer growth [1]–[3]. Using a photodetector, a radiation thermometer determines the temperature of an object by measuring its radiated infrared energy [4]. A narrow band filter is usually employed, to define the wavelength range of the thermometer and minimize the influence of atmospheric attenuation due to water and gas absorption bands. For an accurate measurement using a single-wavelength photodetector, the target emissivity must be well known. In cases where the emissivity is not easily obtained, or when there is additional attenuation caused by the presence of an unwanted medium, such as smoke or steam, a two-wavelength band or a ratio thermometer can be used to correct for the losses. The ratio thermometer works if the emissivity (and the attenuation factor) is the same across the two chosen wavelength bands [4]. In this case, the reduction in signal due to reduced emissivity or attenuation cancels and the ratio of electrical outputs from the two photodetectors is a function of source surface temperature alone [5]. The tandem Si-InGaAs photodetector shows good linearity and can be used for single-spot measurement at temperatures above 400 °C [6]. Hence, the Si-InGaAs photodetector (such as K1713 from Hamamatsu) has been used in a typical single-spot ratio thermometer.

The concept of two-color detection has also been demonstrated to be highly suitable for imaging applications where objects in the imaged scene have different emissivities or are located in an attenuating medium. In some cases, the emissivity changes due to composition variation on the surface, such as growing zinc alloy during galvanneal process and induction skull melting of titanium aluminide [7], [8]. In these situations, it is impossible to translate the measured photocurrent into target temperature if the measurement is performed using a single-waveband detector. Therefore, a radiation thermometry system using a two-color photodetector, which minimizes the influence of emissivity, becomes highly attractive for concomitant temperature sensing and thermal imaging. Yamada *et al.* [9] and Mollmann *et al.* [10] successfully demonstrated a two-color thermal imaging system using an InSb photodetector and narrow-band optical filters. Improved accuracy over conventional thermal camera imaging was obtained using the two-color measurement. Inclusion of filters, such as using of a filter wheel, prevents simultaneous measurement at the wavelengths of interest. Removing the filters can bring further improvements to the two-color imaging, in terms of simpler optical system, reduced cost, and reduced dynamic filters drift and reflections between filters and detector. It is also worth noting that the ratio of signal at the two wavelengths is larger at the shorter wavelength. Therefore, for objects with low emissivities, measurement minimal error is best performed at short wavelengths [11] and two-color measurements are normally performed at selected short wavelengths. For applications with high operating temperature above 400 °C, such as furnace wall-tube

Manuscript received August 1, 2013; revised December 4, 2013; accepted December 27, 2013. Date of current version February 20, 2014. This work was supported in part by Land Instruments Ltd., and in part by The University of Sheffield EPSRC KTA under Contract R/131314 and Contract R/132850. The work of X. Zhou was supported by EPSRC under Grant EP/H031464/1 and studentships from the University of Sheffield. The review of this paper was arranged by Editor E. G. Johnson.

X. Zhou, M. J. Hobbs, B. S. White, J. P. R. David, and C. H. Tan are with the Department of Electronic and Electrical Engineering, The University of Sheffield, Mappin Street, Sheffield S1 3JD, U.K. (e-mail: elq10xz@shef.ac.uk; m.hobbs@shef.ac.uk; ben.white@shef.ac.uk; j.p.david@shef.ac.uk; c.h.tan@shef.ac.uk).

J. R. Willmott is with Land Instruments Ltd., Derbyshire, U.K. (e-mail: jon.willmott@ametek.co.uk).

Color versions of one or more of the figures in this paper are available online at http://ieeexplore.ieee.org.

Digital Object Identifier 10.1109/TED.2013.2297409

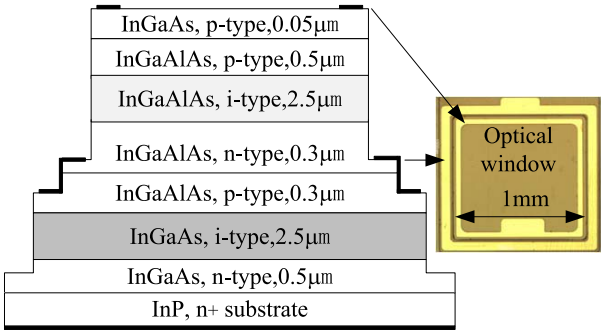

Fig. 1. Cross sectional and top view of the InGaAlAs–InGaAs two-color photodetector.

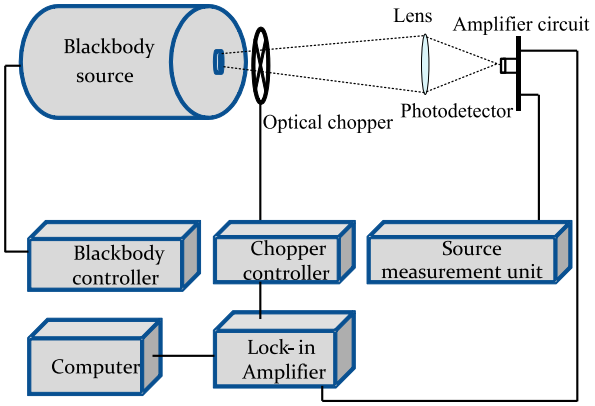

Fig. 2. Setup used to perform thermometry measurement on two-color photodetectors.

monitoring [12] or supervision of low emissivity objects in aluminum industry [13], two-color thermal imagers operating at short wavelengths are desirable.

For a two-color imaging system at the short-wave infrared wavelengths the Si-InGaAs tandem photodetector is not a suitable technology for fabrication of imaging arrays, because the large lattice mismatch of 8% between InGaAs and Si [14] makes epitaxially grown InGaAs on Si impractical and stacking Si diode on InGaAs diode (the approach adopted for Hamamatsu K1713) becomes more complicated for large arrays. On the other hand, the $In_{1-x-y}Ga_xAl_yAs$ quaternary alloy, which is a direct bandgap material, can be easily combined with InGaAs to form two-color imaging arrays grown on high-quality InP substrates. $In_{1-x-y}Ga_xAl_yAs$ also offers several advantages over Si, such as cutoff wavelength tunability from 827 to 1700 nm [15], a higher absorption coefficient, leading to a thinner absorption layer and potential as wavelength tunable multicolor spot thermometer, line scanner, and eventually extremely accurate thermometer camera.

In this paper, we report the first evaluation of an InGaAlAs–InGaAs two-color photodetector for radiation thermometry. The device structure, fabrication details, current– and capacitance–voltage measurements, and the experimental setup are described in Section II. The two-color photodetector characteristics are compared with those of from a commercial two-color photodetector in Section III, followed by a discussion in Section IV and a conclusion in Section V.

II. Experimental Details

A. Device Structure and Fabrication Details

Our two-color photodetector comprises an $In_{0.53}Ga_{0.25}Al_{0.22}As$ (InGaAlAs) p^+in^+ diode, with an alloy composition chosen to achieve a cutoff wavelength of 1100 nm, grown on top of an $In_{0.53}Ga_{0.47}As$ (InGaAs) p^+in^+ diode, which is capable of detecting wavelengths up to 1700 nm. The InGaAlAs–InGaAs structure, shown in Fig. 1, was grown by molecular-beam epitaxy on an InP n^+ conducting substrate at the EPSRC National Center for III–V Technologies at Sheffield.

Mesa devices, shown in Fig. 1, were fabricated using standard photolithography. Mesas were patterned by wet chemical etching using a sulfuric acid: hydrogen peroxide: deionized water (1:8:80) solution. Ti–Pt–Au (10/20/200 nm) metal contacts were deposited on the highly doped InGaAs and InGaAlAs contact layers and the substrate, as shown in Fig. 1. The metal contacts were annealed at 420 °C for 30 s. Surface passivation and antireflection coating on the optical windows were not performed. Three device sizes were fabricated to allow analysis of current density. The top mesa sizes are 1 mm × 1 mm (large), 0.5 mm × 1 mm (medium), and 0.21 mm × 0.235 mm (small), as shown in Fig. 1. The large-area devices were subsequently used for optical measurements. Their optically active areas, calculated by excluding the area shielded by the metal contacts, are 0.84 and 1 mm^2 for the InGaAlAs and InGaAs junctions, respectively.

B. Experimental Details

Current–voltage and capacitance–voltage measurements were performed using an HP4014 picoammeter and an HP4275 LCR meter, respectively. The spectral response of the two-color photodetector was measured using an iHR320 monochromator with a tungsten lamp light source. Diffraction gratings with blaze wavelengths of 1 and 2 μm were used for spectral measurements of the InGaAlAs and InGaAs diodes, respectively. The photocurrents from chopped 1064- and 1550-nm lasers were also measured using a phase-sensitive detection technique [16]. The incident powers onto the device were then measured using an optical power meter, so that the responsivities of both diodes could be calculated. For the radiation thermometry measurements, the setup in Fig. 2 described in [17] was used. We used a calibrated IR-563/301 blackbody source with an emissivity >0.99. The aperture of the blackbody source was set to 10.16 mm in diameter and the photodetector was placed at 300 mm away from the blackbody source. A mechanical chopper was used to modulate the signal from the blackbody at 420 Hz and the modulated signal was focused by a ZnSe lens (Ø1-in Plano-convex lens, $f = 50$ mm) onto the device. The photocurrent from the photodetector was amplified by a transimpedance amplifier circuit with an overall gain of 10^6 V/A. The output signal from the amplifier was recovered using the phase-sensitive detection method by an SR830 lock-in amplifier. This measurement was performed at room temperature and air exposed. The aforementioned commercial

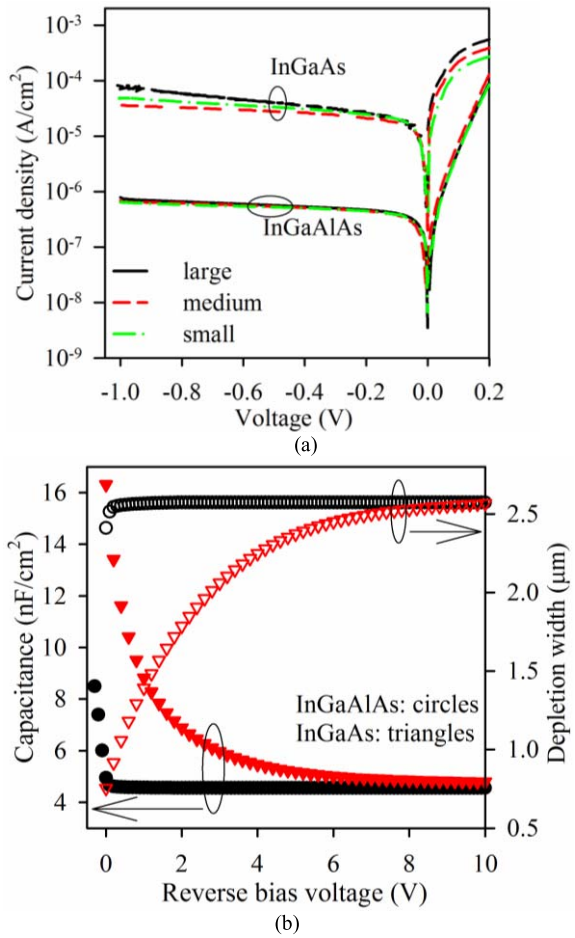

Fig. 3. (a) Dark current density of InGaAlAs and InGaAs diodes. (b) Capacitance and depletion width of InGaAlAs and InGaAs photodetector.

two-color Si-InGaAs photodetector from Hamamatsu, model K1713-09 [18], was used to gauge our photodetector performance in this paper.

III. Result

Fig. 3(a) shows the dark current density of InGaAlAs and InGaAs diodes in this paper. At low biases below 0.1 V, bulk current appears to dominate in both set of diodes. At higher biases, bulk current density of 10^{-6} A/cm^2 was obtained in the InGaAlAs, while the inconsistency of the current density in the InGaAs diodes shows the presence of some surface leakage. The dark currents of both photodetectors are higher than those of commercial diodes suggesting further growth and fabrication improvements are required.

The depletion width as a function of reverse bias was derived from capacitance–voltage measurements shown in Fig. 3(b). The InGaAlAs diode achieves full depletion at 0.1 V while the InGaAs diode is fully depleted at 6 V, suggesting a higher unintentional background doping level in the InGaAs intrinsic region. The depletion widths at 0 V, deduced from the capacitance measurements, are shown in Table I. Parameters from Hamamatsu K1713-09 are also shown for comparison.

The typical reponsivities of our InGaAlAs–InGaAs photodetector and the K1713-09 photodetector at 0 V are shown in Fig. 4. The measured responsivities at 0 V from our diodes

TABLE I
Basic Parameters of Two-Color Photodetectors

Detector	Photodiode material	Active area (mm^2)	Dark current I_d at nominal zero bias (pA)	Depletion width at nominal zero bias (μm)
This work	InGaAlAs	0.84	15	2.41
	InGaAs	1	200	0.75
K1713-09	Si	5.76	<10	10.16
	InGaAs	0.785	<10	0.53

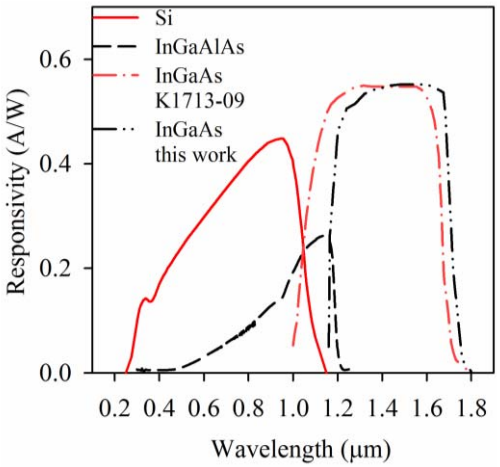

Fig. 4. Responsivity of photodetectors in this paper and commercial K1713-09 photodetector at 0 V.

are 0.25 A/W at 1064 nm for the InGaAlAs diode and 0.55 A/W at 1550 nm for the InGaAs diode. At 1064 nm, the responsivity is lower than 0.44 A/W, measured in the K1713-09(Si) diode, whereas at 1550 nm, it is similar to that in the K1713-09(InGaAs) diode. The InGaAlAs diode shows a cutoff wavelength, defined as 50% of the peak intensity, of 1180 nm (slightly longer than the nominal value targeted), whereas the InGaAs photodetector shows a cutoff wavelength of 1700 nm. These are longer than the cutoff wavelengths of the diodes in K1713-09, most likely due to slight deviation on the alloy composition. Our InGaAs diode also shows a narrower spectrum due to higher absorption of our InGaAlAs in the wavelengths of 1100–1200 nm.

When exposed to the blackbody source, the mean output voltage of the transimpedance amplifier and the signal-to-noise (SNR, taken as the ratio of the mean output voltage to the standard deviation of the output voltage) are shown in Fig. 5. The mean output voltage and the mean SNR were calculated from at least six sets of data, each with more than 2400 experimental data points, taken over 2 min at any given temperature. SNR above 10 was achieved at the lowest measured temperatures of 125 °C and 275 °C for long- and short-band detector, respectively. The mean output voltage and the SNR appear to be comparable with those obtained from commercial detectors in Fig. 5. However, closer inspection reveals that our InGaAlAs diode obtained a slightly higher signal at temperatures below 500 °C but lower signal at temperatures above 500 °C, compared with those measured from K1713-09(Si) diode. The signal from our InGaAs diode

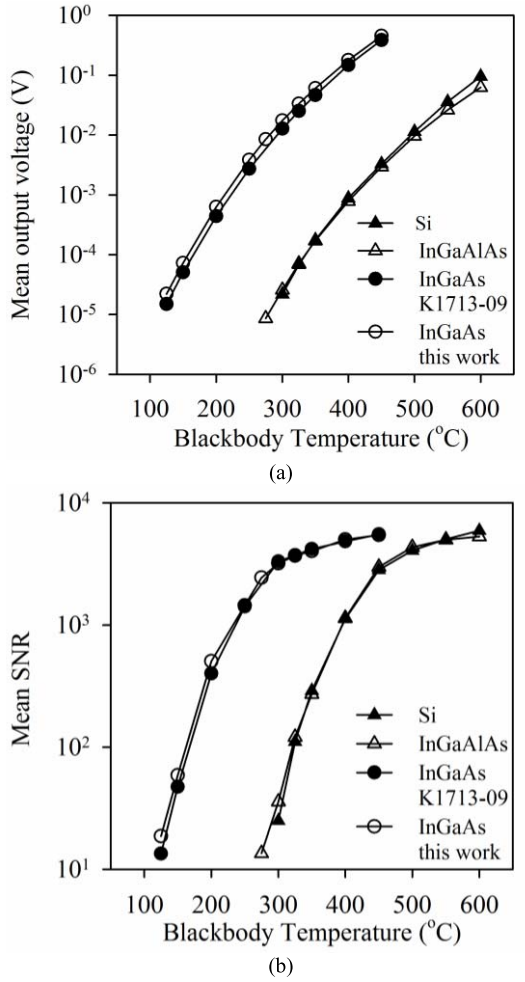

Fig. 5. (a) Mean output voltage and (b) mean SNR of the InGaAlAs–InGaAs photodiode and K1713-09 as a function of the blackbody temperature.

is also slightly higher than that from the K1713-09(InGaAs) diode across the entire temperature range. However, at all measured temperatures, the SNRs from both tandem diodes are similar.

IV. Discussion

The photocurrent from a photodetector can be calculated by integrating the product of the incident optical power with the spectral response of the photodetector. Fig. 6 shows the emitted energy from a blackbody source versus wavelength calculated from Planck's law [19], as well as the Si and the InGaAlAs spectral responses. Longer depletion region width, as shown in Table I, and more efficient carrier collection from the undepleted regions in Si diode gives rise to a higher peak responsivity value than our InGaAlAs diode. We attributed our lower peak responsivity to poor carrier collection efficiency. Carriers generated in the top InGaAs layer are blocked by the p-InGaAlAs layer. The InGaAs layer in the optical window should be removed to improve the quantum efficiency in our diode. Similarly the thickness of the p-InGaAlAs layer can be reduced to improve carrier collection efficiency. Although the responsivity of InGaAlAs is lower than Si at shorter wavelengths, its higher response at

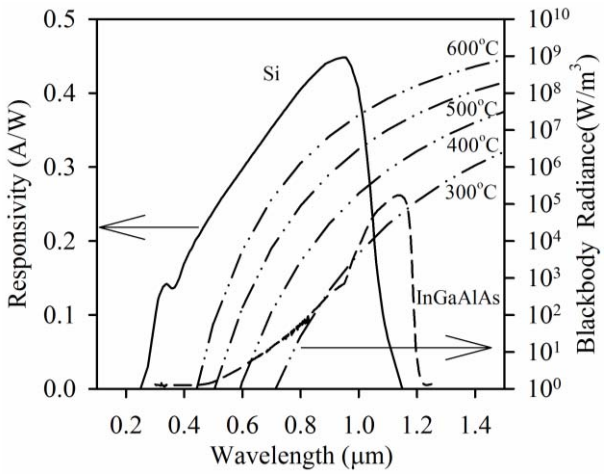

Fig. 6. Si and InGaAlAs spectral responses and spectral radiance of a blackbody at temperatures from 300 °C to 600 °C.

wavelengths above 1100 nm leads to a larger overlap between the diode spectral response and the blackbody radiated spectrum. This larger overlap compensates for the lower response in the shorter wavelength region. Therefore, our InGaAlAs diode produces a slightly higher signal when the radiated power is mostly in the longer infrared wavelengths, when the blackbody temperature is below 500 °C. On the other hand, as the temperature increases, the peak radiated wavelength from the blackbody shifts to a shorter wavelength. Hence, the Si diode, with higher responsivities at shorter wavelengths, produces stronger signal at temperatures above 500 °C, as shown in Fig. 5. The depletion width in our InGaAlAs is 2.41 μm, compared with 10.16 μm in K1713-09(Si). This significantly thinner InGaAlAs is clearly more suitable for development into high-density array than the thick Si. Furthermore, we believe that the responsivity of the InGaAlAs can be increased by optimizing the absorption layer (for instance, by reducing carrier recombination in the p InGaAlAs layer) and inclusion of a broadband antireflection coating. Our InGaAs diode produces higher photocurrent due to a slightly larger area and a longer detection wavelength than the K1713-09(InGaAs) diode.

From Fig. 5, it can be observed that the SNR values are similar for both sets of diode despite our diodes having much higher dark current than their commercial counterparts. This is attributed to the dominance of our amplifier noise over the shot noise from the diode when the photocurrent is low. Using a spectrum analyzer, our amplifier noise of was found to be 125 nV/Hz$^{1/2}$ relatively high compared with state-of-the-art amplifiers. It is also higher than the noise induced by a dark current of 200 pA (equivalent to 8 nV/Hz$^{1/2}$ at the amplifier output) in our InGaAs diode. The SNR increases quickly as the blackbody temperature increases for both tandem diodes. However, the SNRs increase much more gradually at blackbody temperatures above 250 °C and 450 °C for long- and short-wavelength diodes, respectively. These results are consistent with that from [17]. At low blackbody temperatures, the amplifier noise is the dominant noise component in the system; SNR increases as output signal increases rapidly with

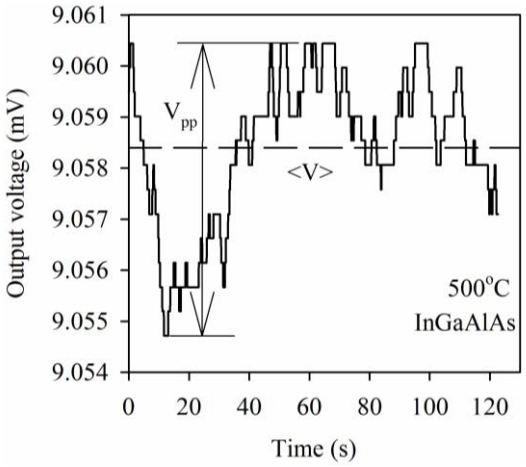

Fig. 7. Fluctuations of output voltage during measurement.

increased temperature. As the blackbody temperature increases to a sufficiently high value, the shot noise induced by the high photocurrent from diode becomes the overwhelming noise source, leading to the observed trend.

The electronic noise of the detector–amplifier combination in the system and influence of laboratory ambience (e.g., temperature and humidity) can be assessed as a temperature error. This value was calculated from the ratio of percentage error of the output voltage to the percentage change in output for a 1 °C rise in the target temperature, known as percent per degree [20], [21]. To assess the error in the output voltage, we measured the largest peak-to-peak voltage (V_{pp}) and the mean output voltage $\langle V \rangle$, as shown in Fig. 7. The percentage error of the output voltage is then defined as $(V_{\mathrm{pp}}/2)/\langle V \rangle$ multiplied by 100, while the percent per degree is given by

$$\%/^{\circ}\mathrm{C} = 100 \times \frac{c_2}{\lambda T^2} \tag{1}$$

where T is the target temperature in kelvin, c_2 is Planck's second constant, 1.4388 cm · K, and λ is the effective operational wavelength of a single-channel thermometer. This effective wavelength is derived from the gradient of the natural logarithm of output voltage plotted as a function of $1/T$ [22], [23]. It is a method based on Wien's law, by approximating broadband wavelengths into a single monochromatic wavelength [24]. The ratio thermometer can be considered to behave in the same way as a single-channel thermometer whose effective wavelength is given by $\lambda = \lambda_1\lambda_2/(\lambda_2 - \lambda_1)$ [4]. Fig. 8(a) shows temperature error for our InGaAs and InGaAlAs diodes and a ratio thermometer. The temperature error ranges from 2.3 °C to 0.02 °C for InGaAs diode and 4 °C to 0.02 °C for the InGaAlAs diode. Hence, the InGaAlAs can be used to measure a blackbody temperature of 275 °C with an uncertainty of 4 °C while the InGaAs diode can measure 125 °C with an uncertainty of 2.3 °C. As a ratio thermometer, this temperature error becomes higher due to longer effective wavelength than single-waveband thermometer. Our two-color thermometer shows an error of 12.8 °C at 275 °C. The error drops with temperature to a value of 0.1 °C at 450 °C. It is well known that the error of a ratio thermometer is larger than a single-wavelength thermometer [21]. Despite this, the importance of a ratio

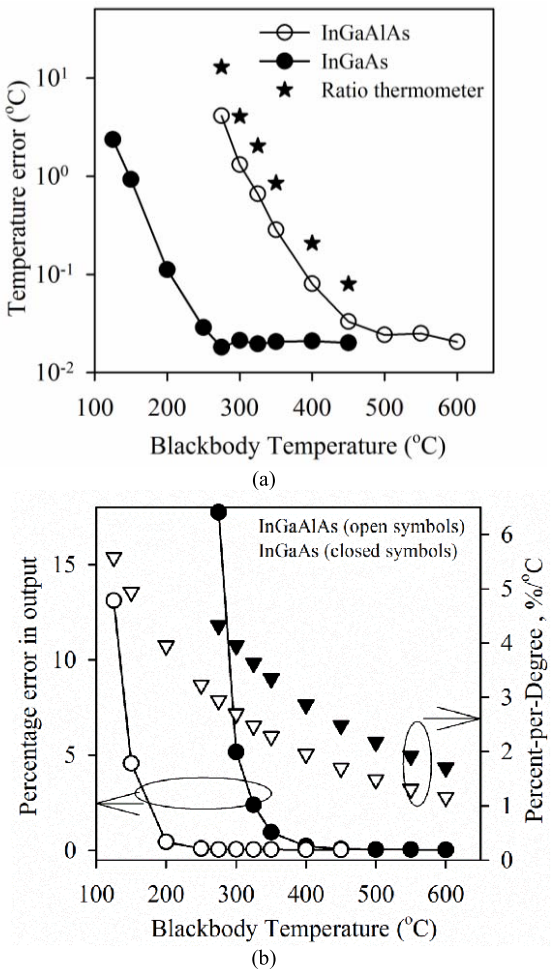

Fig. 8. (a) Temperature error, including electronic noise and laboratory ambience, of the individual diode and when combined as a ratio thermometer and (b) percentage error in output and %/°C at different blackbody temperature.

thermometer in overcoming the measurement errors, due to uncertainties in emissivity and attenuation in the signal path, is well recognized since there is a vast array of manufacturing applications where only measurements of greater than 600 °C are required. When an application dictates that lower temperature measurements are needed, it is possible to achieve this by moving both measurements to longer wavelengths. From Fig. 8, it is clear that the temperature error reduces as blackbody temperature increases. However, it tends to a saturation value of 0.02 °C at temperatures above 250 °C and 450 °C for InGaAs and InGaAlAs, respectively. This is due to the progressively smaller change of percentage error in output signals as temperature increases, which is shown in Fig. 8(b).

With further improvement to increase the responsivity of the InGaAlAs to amplify signal, and lower amplifier noise to reduce total system noise, potentially more sensitive ratio thermometer can be obtained from this material system.

V. Conclusion

In conclusion, we have reported the first evaluation of an InGaAlAs–InGaAs two-color photodetector for use in radiation thermometry. This two-color photodetector achieved comparable output signals with a commercial two-color

Si-InGaAs photodetector. Although the dark currents are higher in our diodes, the SNRs measured are also comparable with the commercial diodes, since the noise is largely dominated by the amplifier when the photocurrent is low. SNR above 10 was achieved at the lowest measured temperatures of 125 °C and 275 °C for long- and short-band detector, respectively. When evaluated as a ratio thermometer, our two-color photodetector shows a temperature error of 12.8 °C at 275 °C, but improves with temperature to 0.1 °C at 450 °C.

VI. Acknowledgment

The diodes were fabricated using facilities within the University of Sheffield EPSRC National Center for III-V Technology.

References

[1] M. Sugiura, Y. Ootani, and M. Nakashima, "Radiation thermometry for high-temperature liquid stream at blast furnace," in *Proc. SICE Annu. Conf.*, Tokyo, Japan, Sep. 2011, pp. 472–475.

[2] B. J. Brosilow, Y. Naor, and Y. Baharav, "Multiple reflection effects during the in-situ calibration of an emissivity independent radiation thermometer," in *Proc. 13th IEEE Int. Conf. Adv. Thermal Process. Semicond.*, Santa Barbara, CA, USA, Oct. 2005, pp. 199–205.

[3] IRCON, Inc., Santa Cruz, CA, USA. (1998, Nov.). *Radiation Thermometry in Molecular Beam Epitaxy* [Online]. Available: http://ircon.com/web/pdf/an110.pdf

[4] J. Dixon, "Radiation thermometry," *J. Phys. E, Sci. Instrum.*, vol. 21, no. 5, pp. 425–436, May 1988.

[5] J. Mishin, M. Vardelle, J. Lesinski, and P. Fauchais, "Two-color pyrometer for the statistical measurement of the surface temperature of particles under thermal plasma conditions," *J. Phys. E, Sci. Instrum.*, vol. 20, no. 6, pp. 620–625, Jun. 1987.

[6] J. Novak and P. Elias, "A silicon-InGaAs tandem photophotodetector for radiation thermometry," *Meas. Sci. Technol.*, vol. 6, no. 10, pp. 1547–1549, Jun. 1995.

[7] G. R. Peacock, "Ratio radiation thermometry thermometers in hot rolling and galvannealing of steel strip," in *Proc. AIP Conf.*, Chicago, IL, USA, Sep. 2003, pp. 789–794.

[8] R. A. Harding and M. Wickins, "Temperature measurements during induction skull melting of titanium aluminide," *Mater. Sci. Technol.*, vol. 19, no. 9, pp. 1235–1246, Sep. 2003.

[9] J. Yamada, T. Murase, and Y. Kurosaki, "Thermal imaging system applying two-color thermometry," *Heat Transf., Asian Res.*, vol. 32, no. 6, pp. 473–488, Sep. 2003.

[10] K. P. Möllmann, F. Pinno, and M. Vollmer, *Two-Color or Ratio Thermal Imaging-Potentials and Limits*. Wilsonville, OR, USA: FLIR Syst., Inc., May 2011.

[11] M. Vollmer and K. P. Möllmann, "Advanced methods in IR imaging," in *Infrared Thermal Imaging: Fundamentals, Research and Applications*. Weinheim, Germany: Wiley, 2011, pp. 164–166.

[12] D. D. Burleigh, K. E. Cramer, and G. R. Peacock, "Furnace wall-tube monitoring with a dual-band portable imaging radiometer," *Proc. SPIE*, vol. 5405, pp. 221–226, Apr. 2004.

[13] B. K. Tsai, D. P. DeWitt, and G. J. Dail, "Application of dual-wavelength radiation thermometry to the aluminum industry," *Measurement*, vol. 11, no. 3, pp. 211–221, Jun. 1993.

[14] N. A. Papanicolaou, G. W. Anderson, A. A. Lliadis, and A. Christou, "Lattice mismatched InGaAs on silicon photodetectors grown by molecular beam epitaxy," *J. Electro. Mater.*, vol. 22, no. 2, pp. 201–206, Feb. 1993.

[15] P. Bhattacharya, "Structural properties of InGaAs," in *Properties of Lattice-Matched and Strained Indium Gallium Arsenide*. London, U.K.: INSPEC, 1993, pp. 20–21.

[16] D. P. Blair and P. H. Sydenham, "Phase sensitive detection as a means to recover signals buried in noise," *J. Phys. E, Sci. Instrum.*, vol. 8, no. 8, pp. 621–627, Aug. 1975.

[17] M. J. Hobbs, C. H. Tan, and J. R. Willmott, "Evaluation of phase sensitive detection method and Si avalanche photodiode for radiation thermometry," *J. Instrum.*, vol. 8, no. 3, p. P03016, Mar. 2013.

[18] Hamamatsu Photonics K. K., Hamamatsu, Japan. (2006, May). *Two-Color Photodetector K1713-05/-08/-09* [Online]. Available: http://www.hamamatsu.com/resources/pdf/ssd/k1713-05_etc_kird1040e03.pdf

[19] S. D. Gunapala and S. V. Bandara, "Quantum well infrared photophotodetector (QWIP) focal plane arrays," in *Intersubband Transitions in Quantum Wells: Physics and Device Applications I*, London, U.K.: Academic, Oct. 1999, pp. 197–282.

[20] J. Taylor. (2010, Aug.). *Infrared Training Notes—Foundation Level*, Land Infrared Int. Ltd., London, U.K. [Online]. Available: http://www.aumico.it/prodotti/files/117.pdf

[21] T. J. Quinn, "Radiation thermometry," in *Temperature*. London, U.K.: Academic, 1990, pp. 332–431.

[22] P. Saunders, "General interpolation equations for the calibration of radiation thermometers," *Metrologia*, vol. 34, no. 3, pp. 201–210, Jun. 1997.

[23] J. W. Hahn and C. Rhee, "Interpolation equation for the calibration of infrared pyrometers," *Metrologia*, vol. 31, no. 1, pp. 27–32, 1994.

[24] P. Saunders, "Uncertainty arising from the use of the mean effective wavelength in realizing ITS-90," in *Proc. AIP Conf.*, vol. 684. 2002, pp. 639–644.

Xinxin Zhou received the B.Eng. degrees from the Department of Electronic and Electrical Engineering, Fujian University of Technology, FuZhou, China, in 2009 and M.Sc. degree in Electronic Engineering from University of Sheffield in 2010. She is currently pursuing the Ph.D. degree with the University of Sheffield, Sheffield, U.K.

Her current research interests include the fabrication and characterization of mid-infrared photodiodes and simulation of high speed device.

Matthew J. Hobbs, photograph and biography not available at the time of publication.

Benjamin S. White, photograph and biography not available at the time of publication.

John P. R. David (SM'96–F'12) received the B.Eng. and Ph.D. degrees from the Department of Electronic and Electrical Engineering, University of Sheffield, Sheffield, U.K., in 1979 and 1983, respectively.

He became responsible for characterization within the SERC (now EPSRC) Central Facility for III–V Semiconductors, University of Sheffield, in 1985. His current research interests include piezoelectric III–V semiconductors and impact ionization in bulk and multilayer structures.

Jon R. Willmott received the Ph.D. degree from the University of Southampton, Southampton, U.K., in 2003.

He has been a Physicist with Land Instruments International Ltd., Dronfield, U.K., since 2004. He is an expert in radiation thermometry, thermal imaging, optical design, instrumentation, and radiometry.

Chee Hing Tan (M'95) received the B.Eng. and Ph.D. degrees in electronic engineering from the Department of Electronic and Electrical Engineering, University of Sheffield, Sheffield, U.K., in 1998 and 2002, respectively.

He has been with the Department of Electronic and Electrical Engineering, University of Sheffield, since 2003, where he is currently a Reader.